International Journal of Luminescence and Applications (ISSN: 2277-6362)
Vol. 5, No. 2, June 2015. Article ID: 087. pp.191-195.

Mechanoluminescence Properties of $Sr_2SiO_4:Dy^{3+}$ Phosphor by Solid State Reaction Method

Ishwar Prasad Sahu[1*], D.P. Bisen[1] and **Raunak Kumar Tamrakar[1]**

[1]*School of Studies in Physics & Astrophysics, Pt. Ravishankar Shukla University, Raipur (C.G.), India*
[2]*Department of Applied Physics, Bhilai Institute of Technology Durg (C.G.), India*

Abstract— *Dysprosium doped di-strontium ortho-silicate namely $Sr_2SiO_4:Dy^{3+}$ phosphor was prepared by the traditional high temperature solid state reaction method. The crystal structure of sintered phosphor was orthorhombic crystallography with space group Pmnb. An EDX spectrum confirm the present elements in $Sr_2SiO_4:Dy^{3+}$ phosphor. The peak of mechanoluminescence (ML) intensity increases linearly with increasing impact velocity of the moving piston. Thus the present investigation indicates that the local piezoelectricity-induced electron bombardment model is responsible to produce ML in prepared $Sr_2SiO_4:Dy^{3+}$ phosphor. The ML decay constant value is increases with the impact velocities, and maximum for the maximum impact velocities.*

Keywords— *XRD;FTIR; Photoluminescence; CIE color cordinates.*

1. INTRODUCTION

Mechanoluminescence (ML) (also known as Triboluminescence) is an important physical phenomenon where an emission of light is observed due to mechanical deformation of materials, when they are subjected to some mechanical stress like rubbing, cleavage, compressing, impulsive deformation, crushing, grinding, shaking etc. This phenomenon has been observed in many kinds of solids including ionic crystals, semiconductors, metals, glasses and organic crystals [1,2]. In the present ML studies, an impulsive deformation technique has been used. During the deformation of a solid, a great number of physical processes may occur within very short time intervals, which may excite or stimulate the process of photon emission. When a moving piston is applied to the phosphor, initially the ML intensity increases with time, attains a peak value and then decreases with time. Such a curve between the ML intensity and deformation time of phosphors is known as the ML glow curve [3, 4].

ML has found various important applications such as impact sensors in spacecrafts (the emission intensity can be used to determine the kinetic energy of impact), fracture sensor, damage sensor, stress sensor etc. Thus, many researchers have been focused on the investigation of phosphors with high ML [5]. Until now, some phosphors with high ML, such as (red phosphor) $BaTiO_3$–$CaTiO_3$:Pr, (green phosphor) $SrAl_2O_4$:Eu, (yellow phosphor) ZnS:Mn, and (blue phosphor) $CaYAl_3O_7$:Eu etc., have been developed. However, the requirement of application for ML sensors still is not satisfied with the development of ML materials. At the same time, the high stabilities, such as resistance of water, thermal stability are also very important for the application of ML. More ML phosphors with strong ML intensity and high stability are needed [6-8].

It is well known that silicates have a higher physical and chemical stability after water treatment. Therefore, in this paper, we report the synthesis of dysprosium doped di-strontium ortho-silicate phosphor by high temperature solid state reaction method. This paper reports the structural characterization on the basis of XRD and EDX analysis and studies of optical properties are also investigated on the basis of mechanoluminescence (ML).

2. EXPERIMENTAL

2.1 Material Preparation

The dysprosium doped strontium silicate white light emitting phosphor was synthesized by solid state reaction method. The starting materials were strontium carbonate [$SrCO_3$ (99.90%)], silicon di-oxide [SiO_2 (99.99%)], and dysprosium oxide [Dy_2O_3 (99.99%)], all of analytical grade (A.R.), employed in this experiment. Small amount of Boric acid (H_3BO_3) was added as flux. Initially, the raw materials were weighed according to the nominal compositions of $Sr_2SiO_4:Dy^{3+}$ phosphor, then the powders were mixed and milled thoroughly for 2 hour using agate mortar and pestle. The chemical reaction used for stoichiometric calculation is:

$$2SrCO_3 + SiO_2 + Dy_2O_3 \rightarrow Sr_2SiO_4:Dy^{3+} + 2CO_2\uparrow$$

The ground sample was placed in an alumina crucible and subsequently fired at 1200°C for 3 hours in an air. At last the nominal compounds were obtained after the cooling down of programmable furnace and products were finally ground into powder for characterizing the phosphors. Solid state reaction method is widely used to prepare silicate based phosphors because samples prepared using

* *Corresponding Author Email: ishwarprasad1986@gmail.com*

this method has good luminescence and very good morphology.

3. CHARACTERIZATION TECHNIQUES

The crystal structures of the prepared $Sr_2SiO_4:Dy^{3+}$ phosphor was characterized by powder XRD analysis. Powder XRD pattern has been obtained from Bruker D8 advanced X-ray powder diffractometer using CuKα (1.54060 Å) radiation and the data were collected over the 2θ range 10-80°. The structure of the sample was verified with the help of Joint Committee of Powder Diffraction Standard Data (JCPDS) file (JCPDS: 17-1630). Energy dispersive x-ray spectroscopy (EDX) was used for the elemental analysis of the prepared phosphor. The ML measurement was observed by the home made lab system comprising of an RCA-931A photomultiplier tube (PMT). The ML glow curve can be plotted with the help of SM-340 application software installed in a computer attached with the storage oscilloscope. All measurements were carried out at the room temperature.

4. EXPERIMENTAL SETUP FOR MECHANOLUMINESCENCE (ML) MEASUREMENT

The experimental set up used for the impulsive deformation of ML was shown in Fig.1. A load (moving piston) of particular mass and shape was dropped from different heights [different impact velocities (υ_0)] for striking the prepared $Sr_2SiO_4:Dy^{3+}$ phosphor. In this experiment, the mass of the dropping load was 400 g and shape of the load was cylindrical. The phosphor under study was placed on the upper surface of a transparent lucite plate and it was then covered with a thin aluminum foil and fixed with an adhesive tape. The foil reflects light and prevents scattering of the fragments during the impact of a moving piston onto the prepared phosphor. This arrangement eliminates the error in the ML measurement due to the scattering of the crystallite fragments during the impact of the load onto the phosphor. The housing is made up of thick soft iron to provide shielding from light and magnetic field. The slit arrangement at the window is provided to adjust the size of the window according to the incident beam. When the phosphor placed on the lucite plate was crushed by impact of the moving piston, light is emitted [9].

By changing the distance between the moving piston to be dropped and the sample placed on the lucite plate, the impact velocity of the load, could be changed from 198 cm/s to 313 cm/s (20 to 50 cm height). Since the pulley and the guiding cylinder used were of negligible friction, the impact velocity was taken as $\sqrt{2gh}$, where "g" is the acceleration due to gravity and "h" is the height through which the moving piston is dropped freely. An RCA 931A photomultiplier tube (PMT) was placed below the transparent lucite plate. The PMT was run at 750 Volts. The output of photomultiplier tube was connected to the phosphorescent screen oscilloscope (Scientific 300 MHz, SM 340). The ML glow curve can be plotted with the help of SM-340 application software installed in a computer attached with the storage oscilloscope [10].

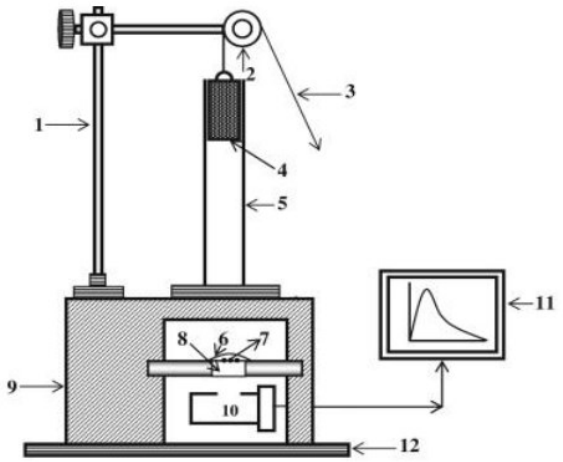

Fig. 1: Schematic diagram of the experimental setup for ML measurement

In the Fig. 1, 1 - Stand; 2 - Pulley; 3 - Metallic wire; 4 - Load; 5 - Guiding cylinder; 6 - Aluminium foil; 7 - Phosphor; 8 - Transparent Lucite plate; 9 - Wooden block; 10 - Photomultiplier tube (PMT); 11 - Storage oscilloscope; 12 - Iron base mounted on a table.

5. RESULTS AND DISCUSSION

5.1 XRD Analysis

In order to determine the crystal structure, powder XRD analysis has been carried out. The typical XRD patterns of $Sr_2SiO_4:Dy^{3+}$ with that of the standard JCPDS file are shown in Fig. 2. Nearly, all the diffraction peaks of the resultant phosphor are consistent with Joint Committee Powder Diffraction Standard data (JCPDS) file (JCPDS: 17-1630). The position and intensity of diffraction peaks of $Sr_2SiO_4:Dy^{3+}$ are well matched with the standard JCPDS file. The crystal structure for observed XRD

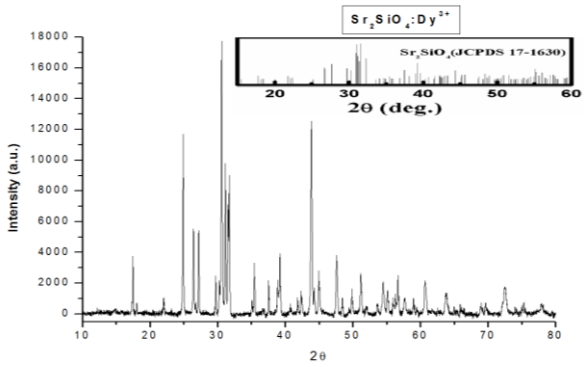

Fig. 2: XRD pattern of $Sr_2SiO_4:Dy^{3+}$ phosphor

patterns were consistent with the orthorhombic crystallogtaphy with space group Pmnb. The small amount of impurity did not change the crystal ctructure of the sintered phosphor. The radius of Dy^{3+} (0.99 Å) are very close to that of Sr^{2+} (about 1.12 Å) rather than Mg^{2+} (0.65 Å) and Si^{4+} (0.41 Å). Therefore, the Dy^{3+} ions are expected to occupy the Sr^{2+} sites in the $Sr_2SiO_4:Dy^{3+}$.

5.2 Energy Dispersive X-Ray Spectroscopy (EDX)

Fig. 3 shows the EDX spectra of $Sr_2SiO_4:Dy^{3+}$ phosphor. The composition of the powder sample has been measured using EDX. Table 1 shows the compositional elements of $Sr_2SiO_4:Dy^{3+}$ phosphor, which is compare with the standard element. Energy dispersive x-ray spectroscopy (EDX) is a standard procedure for identifying and quantifying elemental composition of sample area as small as a few nanometers. Their appeared no other emissions apart from strontium (Sr), silicon (Si), oxygen (O) and dysprosium (Dy) in EDX spectra of the sample. In the spectrum intense peaks are present which confirm the formation of $Sr_2SiO_4:Dy^{3+}$ phosphor.

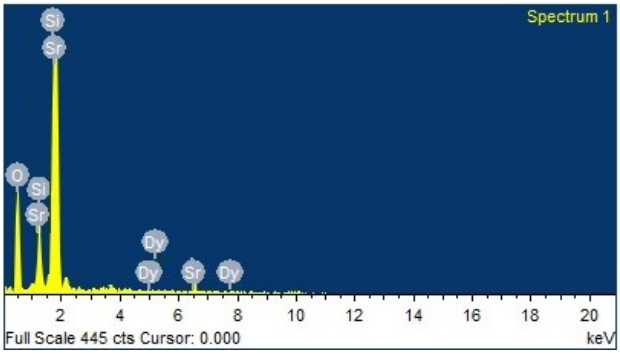

Fig. 3: EDX spectra of $Sr_2SiO_4:Dy^{3+}$ phosphor

Table 1: Composite element of $Sr_2SiO_4:Dy^{3+}$ phosphor

S.N.	*Standard*	*Elements*	*Atomic(%)*	*Weight(%)*
1	SiO_2	O K	42.41	57.17
2	SiO_2	Si K	15.54	14.67
3	SrF_2	Ca L	33.18	25.85
4	DyF_3	Dy L	8.86	2.30
Total			99.99	99.99

5.3 Mechanoluminescence (ML)

Fig. 4 shows that the characteristics curve between ML intensity versus time for different heights (h = 20, 30, 40, 50 cm). The phosphor was fracture via dropping a load [moving piston] of particular mass (400 g) and cylindrical shape on the $Sr_2SiO_4:Dy^{3+}$ phosphor. The velocity of the moving piston, holding the impact mass, could be changed, by changing the height through which it was dropped. Every time for the ML measurement, the quantity of $Sr_2SiO_4:Dy^{3+}$ phosphor was kept constant (8 mg). When the moving piston is dropped onto the prepared phosphor at different height, light is emitted. The photon emission time is nearly 2 ms, when prepared $Sr_2SiO_4:Dy^{3+}$ phosphor fractures. In these ML measurements, maximum ML intensity has been obtained for the 50 cm dropping height and ML intensity increases linearly with the increases the falling height of the moving piston. The sintered $Sr_2SiO_4:Dy^{3+}$ phosphor was not irradiated by any excitation source [11].

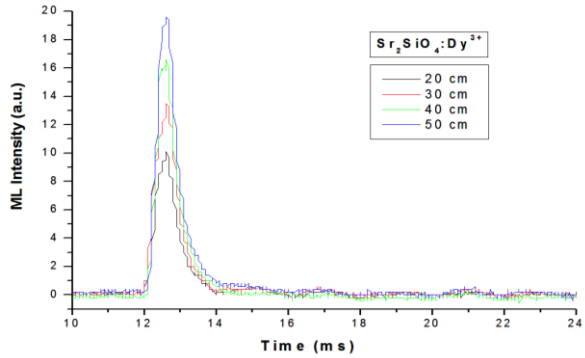

Fig. 4: ML intensity versus time curve of $Sr_2SiO_4:Dy^{3+}$ phosphor

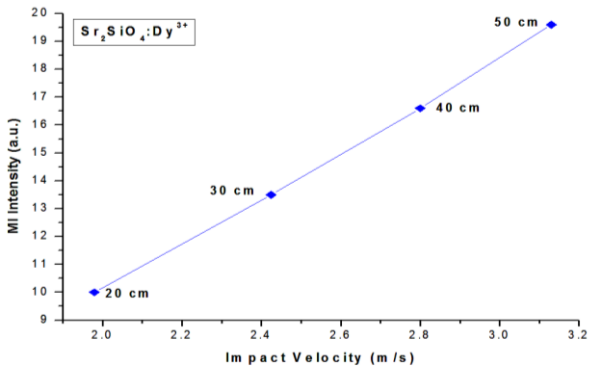

Fig. 5: ML intensity versus impact velocity curve of $Sr_2SiO_4:Dy^{3+}$ phosphor

Fig. 5 shows the characteristics curve of ML intensity versus impact velocities for $Sr_2SiO_4:Dy^{3+}$ phosphor. It is seen that, ML intensity increases linearly with increasing

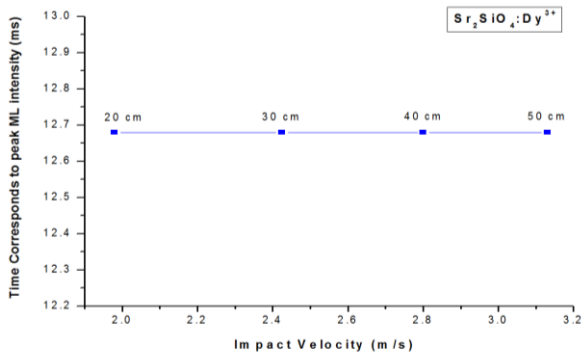

Fig. 6: Time corresponds to ML signal peak with impact velocity of $Sr_2SiO_4:Dy^{3+}$ phosphor

impact velocity [$\sqrt{2gh}$, (where "g" is the acceleration due to gravity and "h" is the height through which the load is dropped freely)] of the moving piston. The ML intensity of $Sr_2SiO_4:Dy^{3+}$ phosphor increases linearly with increasing the mechanical stress [12].

Fig. 6 shows the time corresponds to ML signal peak with impact velocity of $Sr_2SiO_4:Dy^{3+}$ phosphor. It can be seen that time for peak ML intensity does not change significantly with increasing impact velocity. The relationship between semi-log plot of ML intensity versus ($t–t_m$) for $Sr_2SiO_4:Dy^{3+}$ phosphor is shown in Fig. 7, and the lines were fitted using the following equation with Origin 8.0

$$\tau = \frac{1}{slop\ of\ straight\ line}$$

Curve fitting results show that decay constant (τ) varies from 0.86 to 0.93 ms. The ML decay constant value is increases with the impact velocities, and maximum for the maximum impact velocities (See table 2).

Table 2: Calculation of ML decay constant

Impact velocity	20 cm	30 cm	40 cm	50 cm
Decay constant (ms)	0.86	0.88	0.90	0.93

When a mechanical stress, such as compress, friction, and striking, and so on, was applied on the sintered $Sr_2SiO_4:Dy^{3+}$ phosphors, piezo-electric field can be produced. Therefore, in such phosphor the ML excitation may be caused by the local piezoelectric field near the impurities and defects in the crystals. During the impact on the material, one of its newly created surfaces gets positively charged and the other surface of the crack gets negatively charged. Thus, an intense electric field of the order of 10^6 - 10^7 Volt cm^{-1} is produced.

Under such order of electric field, the ejected electrons from the negatively charged surface may be accelerated and subsequently their impact on the positively charged surfaces may excite the luminescence center such as Dy^{3+} [13]. Subsequently, the de-excitation of excited Dy^{3+} ions may give rise to the light emission due to the transition from excited state to ground state.

With the increasing impact velocity, more compression of the sample takes place, and therefore, more area of the newly created surface takes place. Thus, the ML intensity will increase with increasing value of the impact velocity. It is to be noted that the stress near the tip of a moving crack is of the order of $Y/100 \approx 10^{10}$ dynes/cm^2 = 10^9 Newton/m^2 (where Y is the Young's modulus of the materials). Thus, a fixed charge density will be produced on the newly created surfaces and the increase in the ML intensity will primarily be caused by the increase in the rate of newly created surface area with increasing impact velocity. Moreover, the total ML intensity will also increase with impact velocity because more compression of the sample will create more surfaces with increasing impact velocity.

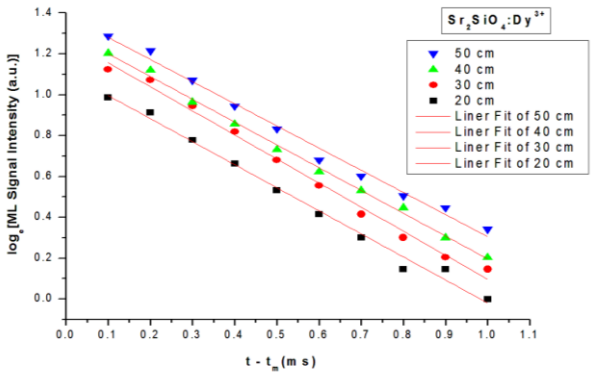

Fig. 7: Semi-log plot of ML intensity versus ($t – t_m$) for $Sr_2SiO_4:Dy^{3+}$ phosphor

As the impact velocity increases, the impact pressure also increases leading to the increase in the electric field at local region which causes the decrease in trap depth. Hence the probability of de-trapping increases. From Fig. 5, it can be seen that with increasing impact velocity, ML intensity also increases linearly i.e., the ML intensity of $Sr_2SiO_4:Dy^{3+}$ phosphor are lineally proportional to the magnitude of the impact velocity, which suggests that this phosphor can be used as sensors to detect the stress of an object [14].

6. CONCLUSION

In summary, the $Sr_2SiO_4:Dy^{3+}$phosphor was prepared by the traditional high temperature solid state reaction method. The crystal structure of the $Sr_2SiO_4:Dy^{3+}$ phosphor is consistent with standard consistent with the orthorhombic crystallogtaphy with space group Pmnb. The radius of Dy^{3+} (0.99 Å) are very close to that of Sr^{2+} (about 1.12 Å) rather than Mg^{2+} (0.65 Å) and Si^{4+} (0.41 Å). Therefore, the Dy^{3+} ions are expected to occupy the Sr^{2+} sites in the $Sr_2SiO_4:Dy^{3+}$. An EDX spectrum confirm the present elements in $Sr_2SiO_4:Dy^{3+}$ phosphor.It should be noted that the dependences between ML intensities and loads are close to linearity, which suggests that these phosphor can be used as sensors to detect the stress of an object.

REFERENCES

[1] D.R. Vij, Luminescence of Solids, Plenum Press, New York (1998).

[2] C. N. Xu, T. Wantanabe, M. Akiyama, and X. G. Zheng, Appl. Phys. Lett. 1999; 74: 1236 – 1238.

[3] C. N. Xu, T. Wantanabe, M. Akiyama, and X. G. Zheng, Mater. Res. Bull. 1999; 34: 1491-1500.

[4] C. N. Xu, T. Wantanabe, M. Akiyama, and X. G. Zheng, Appl. Phys. Lett. 1999; 74: 2414-2416.

[5] C. N. Xu, X. G. Zheng, M. Akiyama, K. Nonaka, and T. Wantanabe, Appl. Phys. Lett. 2000; 76: 179 – 181

[6] C. N. Xu, X. G. Zheng, T. Wantanabe, M. Akiyama, I. Usui, Thin Solid Films 1999; 352: 273 -278.

[7] I. P. Sahu, D. P. Bisen, N. Brahme, Displays 2015; 38: 68 - 76.

[8] I. P. Sahu, D. P. Bisen, N. Brahme, Lumin. J. Biol. Chem. Lumin. (2014) http://dx.doi.org /10.1002/ bio.2771.

[9] I. P. Sahu, D. P. Bisen, N. Brahme, Displays, 2014; 35: 279 – 286.

[10] I. P. Sahu, D. P. Bisen, N. Brahme, L. Wanjari, R. K. Tamrakar, Res. Chem. Intermed. (2015) DOI:10.1007/s11164-015-1929-1.

[11] Zhang H, Yamada H, Terasaki N, Xu C N, Int. J. Mod Phys B, 2009; 23 (6-7): 1028 – 1033.

[12] H. Zhang, H. Yamada, N. Terasaki, C.N. Xu, Thin Solid Films 518 610 – 613 (2009).

[13] B. P. Chandra, A. K. Rathore, Cryst. Res. Tech. 1995; 30 (7): 885 - 896.

[14] H. Zhang, H. Yamada, N. Terasaki, C.N. Xu, Physics E 42 2872 – 2875 (2010).